Modular synthesis of nimbolide and its analogues as PARP1 trapping inducers

Authors: Heping Deng,[1†] Hejun Deng,[1†] Chiho Kim,[1,2] Peng Li,[1] Xudong Wang,[1,2] Yonghao Yu,[1,2] and Tian Qin[1]*

Affiliations:

[1] Department of Biochemistry, The University of Texas Southwestern Medical Center, 5323 Harry Hines Blvd, Dallas, Texas, 75390, United States.

[2] Present address: Department of Molecular Pharmacology and Therapeutics, Columbia University Irving Medical Center, New York, NY 10032, USA.

* Correspondence to: tian.qin@utsouthwestern.edu.

† These authors contributed equally to this work.

Abstract:

PARP1 inhibitors (PARPi) has reshaped the clinical treatment of cancer patients with germline *BRCA1/2* mutations presumably due to their ability to induce PARP1 trapping. Since PARPi resistance is frequently observed, there is still an unmet need to develop next generation PARP1-targeting agents for a more complete and sustained therapeutic effect. Historically, natural products have played pivotal roles in anticancer drug development by providing novel targets and mechanism of actions. In our recent discovery[20], a ring seco-C limonoid natural product, nimbolide, was found to inhibit a Poly-ADP-Ribosylation (PARylation)-dependent ubiquitin E3 ligase RNF114, and in doing so, induce the "super trapping" of both PARylated PARP1 and PAR-dependent DNA repair factors. Modular access to nimbolide and its analogues represents an opportunity to develop novel agents as the second generation PARP1-targeting agents for the treatment of *BRCA*-deficient cancers. Here, we report a convergent synthesis of nimbolide through a pharmacophore-directed, late-stage coupling strategy. The broad generality of this route is demonstrated through the synthesis of a variety of analogues with their preliminary cellular cytotoxicity and PARP1 trapping activity reported.

Main text:

Cancer continues to be a major cause of morbidity and mortality[1]. In the past decades, taking advantage of the concept of synthetic lethality[2], PARP1 (Poly-ADP-ribose Polymerase 1) inhibitors (PARPi) have radically reshaped the clinical treatment of cancer patients with germline *BRCA1/2* mutations[3-5]. To date, four PARPi (see Figure 1A) have received the FDA approval for the treatment of *BRCA1/2*-mutated ovarian cancers (and/or breast, prostate, pancreatic cancer)[6]. All of these PARPi bind to PARP1 through mimicking the primary amide group in the cofactor NAD^+ (nicotinamide adenine dinucleotide). It was initially thought that PARPi kill tumor cells by inhibiting the catalytic activity of PARP1 and thus blocking PARylation[7] (Poly-ADP-ribosylation)-dependent DDR (DNA damage response) signaling[8]. More recent studies showed that besides inhibiting PARP1, the FDA-approved PARPi all possess a second activity, namely, to induce PARP1 trapping[9-13]. Specifically, it has been shown that PARP1 is recruited to DNA lesions at the early stage of DDR. In the presence of a PARPi, PARP1, however, is retained at the DNA damage site for an extended period of time (PARP1

trapping) (Figure 1B). It has been shown that PARP1 trapping plays a key role in mediating the DNA damage, cytotoxicity and innate immunomodulatory functions of PARPi.[9-13]

Despite these progresses, the intrinsic and acquired resistance to PARPi underscores the critical need to develop next generation PARPi with distinct mechanism of action (MOA)[14]. Historically, natural products have played pivotal roles in human health by providing active ingredients of folklore medicine.[15] The intriguing structural-topological features of these complex secondary metabolites coupled with their unique biological properties have spawned widespread interests in the chemistry community[16-19]. In our accompanying report[20], we identified RNF114 as a PARylation-dependent ubiquitin E3 ligase. In a landmark disclosure by Nomura and Maimone[21], a ring seco-C limonoid natural product nimbolide[22] was identified as a covalent inhibitor of RNF114. We found that by pharmacologically blocking the ubiquitin E3 ligase activity of RNF114, nimbolide is able to induce a profound level of PARP1 trapping.[20] Importantly, in contrast to conventional PARPi (these compounds trap PARP1), nimbolide treatment leads to the trapping of both PARP1 and PAR-dependent DNA repair factors[20] (e.g., XRCC1)[23]. This "super trapping" activity of nimbolide translates into its superior activity to kill cancer cells with *BRCA* mutations (Figure 1B). Furthermore, nimbolide is also able to overcome intrinsic and acquired resistance to PARPi[20]. The details of these mechanisms are described in reference 20. Inspired by recent successes in the development of rapid synthesis to bioactive terpenoids[24-26] and in order to identify the nimbolide analogues ("super natural product")[27] with improved potency, a flexible and modular synthetic route towards nimbolide was deemed imperative and valuable.

To maximize the potential scope of the nimbolide analogues, a convergent pharmacophore-directed late-stage coupling strategy was envisioned to access the nimbolide scaffold[28]. Based on covalent-binding property of nimbolide and our preliminary studies,[20] the enone moiety and lactone ring of nimbolide were considered as the essential pharmacophore for the observed activity (Figure 1C)[20]. We surmised that nimbolide and its synthetic derivatives **9** could be rapidly accessed from the pharmacophore-contained building block **7** and the modular unit **8**. Despite the straightforward retrosynthetic analysis, identification of robust, versatile functional groups tolerated and scalable strategy to forge these bonds is not trivial. After considerable exploration, the fragments **10** and **11** were identified and realized in the nimbolide synthesis. Our synthesis represents the first total syntheses of nimbolide and several related ring seco-C limonoids natural products[29, 30]. The medicinal-chemistry relevance of this route is demonstrated through divergent synthesis of a variety of analogues.

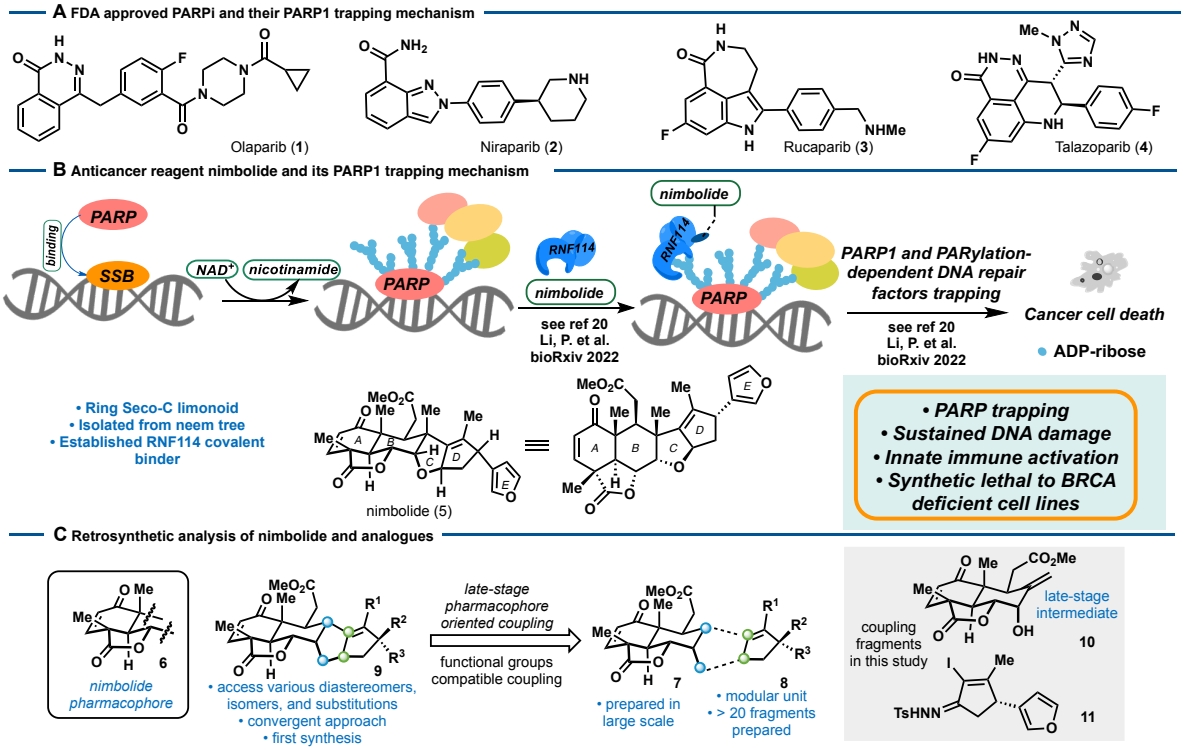

Figure 1. Anticancer reagent nimbolide as PARP1 trapping inducer and retrosynthetic analysis. (**A**) Current FDA approved PARPi and their PARP trapping mechanism; (**B**) The limonoid nimbolide and its PARP1 trapping mechanism; The nimbolide-induced PARP1 trapping mechanism was discovered and elaborated in ref 20. (**C**) Pharmacophore-derived retrosynthetic analysis of nimbolide and analogues.

As outlined in Figure 2, our synthesis began with the reported ketone **12**, which was prepared on >350 gram scale from abietic acid or dehydroabietic acid (see Supporting information)[31-33]. Treatment of **12** with catalytic Pd-mediated Saegusa oxidation[35] followed by dihydroxylation and TMS protection gave the protected diol **14** as a single diastereomer on deca-gram scale. Initial TFDO C–H oxidation[36] on the unprotected lactone **30**[37] resulted in hydrate **31** as the major product, along with the C2 and C1 oxidizing products **32** and **33** in low yields (Figure 2, Part C). However, after thorough investigation of the substrates and conditions, a gram-scale TFDO C–H oxidation was realized on substrate **14** to afford the desired C-2 ketone **15** in a 53% yield, and the C-3 ketone **15** in a 12% yield[38] (see Supporting information for optimization details). The sequent reduction of ketone to olefin **17** was unexpectedly challenging. Most of the conditions (such as Martin sulfurane or Burgess reagent) only provided the undesired alkene product **18**. Gratifyingly, the one-pot Bamford-Stevens reduction generated the olefin **17** with decent yield. The olefin **17** was also prepared from the C3-ketone **16** in a similar manner with 66% yield. With the olefin **17** in hand, the core **10** was smoothly synthesized through a sequence of Wittig olefination, lactonization, SeO_2-mediated allylic oxidation[39] and TES group deprotection. The chemical structure of **10** was unambiguously assigned through single crystal X-ray diffraction analysis. The robustness of this synthetic route was demonstrated by the gram-scale preparation of **10**, which facilitated the modular access towards nimbolide analogues with versatile architectures.

For the preparation of the cyclopentenone fragment **29**, several distinct synthetic routes were investigated. Despite the racemic synthesis of cyclopentenone **29** was achieved through nickel-mediated Fischer carbene cross-couplings in our early trials[40], the asymmetric synthesis

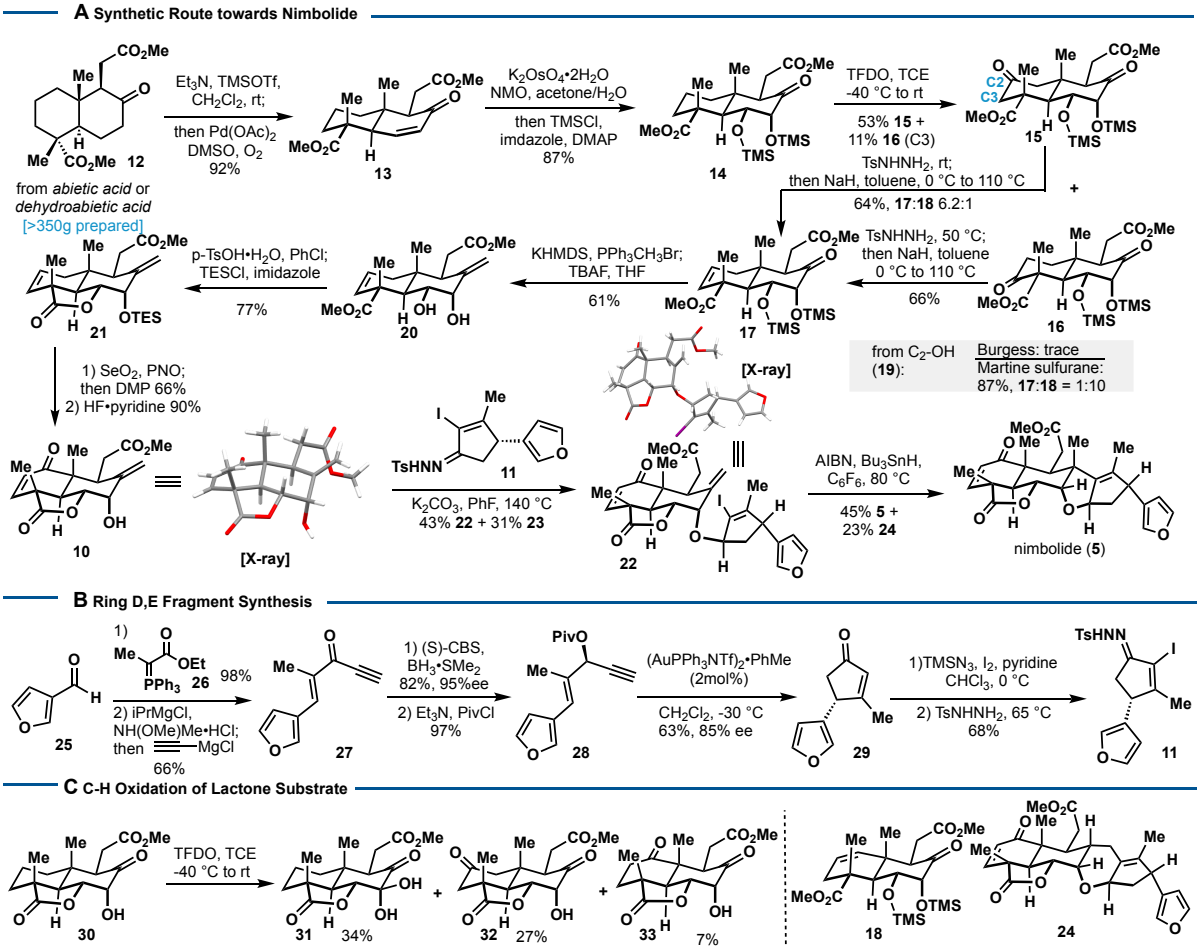

Figure 2. Fragments preparation and synthetic route towards nimbolide.

was unfruitful[41-43]. Subsequent attempts installing the chirality using CBS-reduction and preparation of cyclopentanone via Rautenstrauch rearrangement allowed for asymmetric synthesis of **29** in 7 steps from 3-furaldehyde **25**. As illustrated in Figure 2B, starting from furan ester **25**, the ketone **27** with terminal alkyne was accessed. The CBS reduction generated the chiral alcohol in 89% yield and 95% *ee*. After installing the pivalate group (**28**), the key gold-catalyzed Rautenstrauch rearrangement[44] was screened and optimized to provide the chiral enone **29** in a 63% yield and 85% *ee* (optimization see Supporting Information for details). The α-iodo installation was enabled under the treatment of $TMSN_3$ and I_2[45] and the sulfonyl hydrazone **11** smoothly obtained through condensation with tosyl hydrazide.

With these two advanced building blocks in hand, the ether coupling was investigated between **10** and cyclopentenone derivatives. A series of distinct strategies have been examined for this ether bond formation. However, S_N2/ S_N2' substitution, transition-metal mediated coupling or tethered approach all failed to forge the desired ether bond (see Supporting Information for details). Through a series of optimization, we eventually applied the sulfonyl hydrazone-mediated etherification between **10** and **11**[46,47]. Fortunately, the desired ether products (**22** and **23**) were obtained in high yields with *1.4:1 dr*, favoring the correct stereochemical diastereomer. Thus, we turned our attention towards the last cyclization step. During our model studies, the desired cyclized products (**36, 37**) were isolated through Fe-H mediated radical *ipso* substitution (Figure 3A)[48]. However, this cyclization failed in the real system, presumably due to the additional strains. After extensive screenings, the 5-*exo* cyclized nimbolide (**5**) was obtained as the major product under the treatment of AIBN/nBu$_3$SnH condition (Figure 2). The implementation of hexafluorobenzene as a solvent proved to be

crucial for favoring the 5-*exo* cyclized product instead of protodeiodination and 6-*endo* product **24**[49]. On applying the same conditions to the diastereomer **23**, 6-*endo* cyclization was the only isolated product (**40**, Figure 3B). It is noteworthy that the Pd-mediated cyclization was also investigated (Figure 3C) but only the strained product **41** was isolated in a high yield, through a sequential 5-*exo*/3-*exo* Heck reaction[50].

The successful preparation of nimbolide enabled us to access other related limonoids natural products (Figure 4). Subjecting nimbolide (**5**) to the Mn-H reductive conditions[51], reduced the enone to obtain 2,3-dihydronimbolide (**42**)[52]. The open-lactone natural product, 6-deacetylnimbin (**45**)[53] was accessed quantitatively under the treatment of sodium methoxide. On exposure to LiOH•H_2O and mild heat (60 °C) conditions, 6-deacetylnimbinene (**43**)[54] was accessed through decarboxylation and protonation at the α-position. Lastly, the downstream acetylated natural products nimbin (**46**)[53] and nimbinene (**44**)[54] were synthesized in high yields with acetylation conditions.

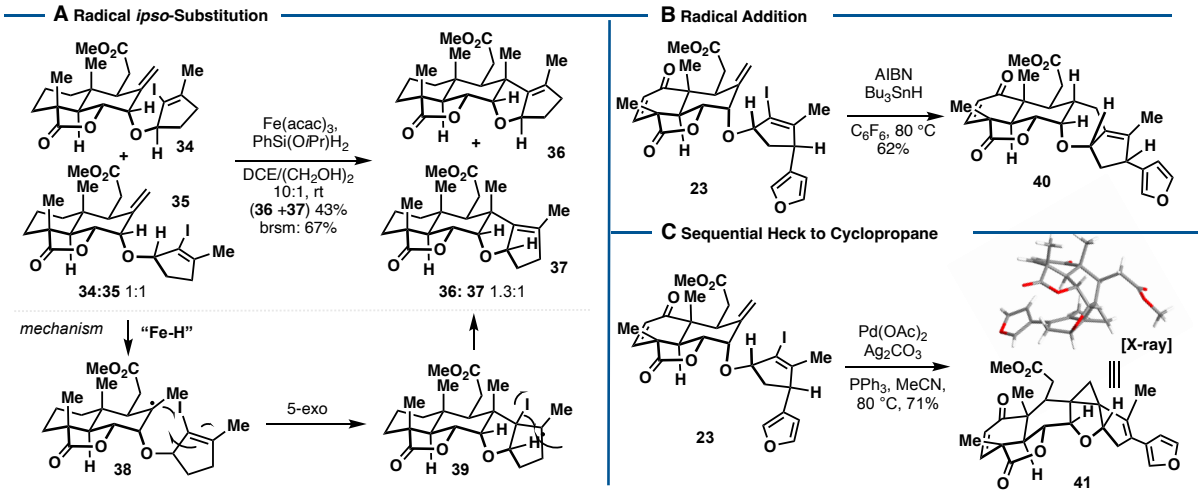

Figure 3. Model studies and cyclization. (**A**) Iron hydride mediated radical *ipso*-substitution; (**B**) Radical 6-*endo* cyclization on substrate **23**; (**C**) Pd-catalyzed Heck cyclization.

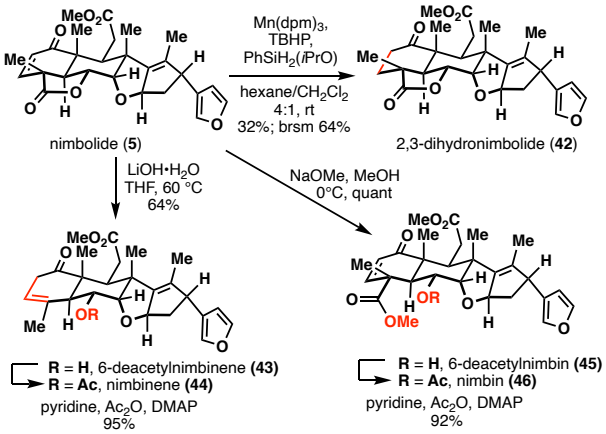

Figure 4. Late-stage diversification of nimbolide for synthesis of related limonoid natural products.

Based on the proposed MOA, nimbolide's superior PARP trapping efficacy relies on its subtle interaction with RNF114, inhibiting the E3 ligase activity while maintaining the substrate binding of RNF114 to the PARylated PARP1. To leverage this discovery and probe RNF114 as a novel potential drug target, the ideal small molecule is required not only to be a selective inhibitor of RNF114, but also to act specifically without interfering the PAR binding

affinity. Facing these joint challenges and with our established synthetic route, we envisage to systematically investigate analogues targeting RNF114 commencing from lead compound nimbolide. The cellular cytotoxicity of nimbolide-derived nature products as well as truncated intermediates and isomers from our synthetic route were studied against UWB1 cell line, which is a *BRCA1*-deficient ovarian cancer cell line. Nimbolide-derived products without enone (**42**, **43**, **44**, **61**) or lactone motif (**45**, **46**) demonstrate minimal cytotoxicity (>10 μM) while the synthetic intermediate **60** with the A and B ring in place still exhibits cytotoxicity. These results indicate that the enone group and the lactone across the A and B ring is crucial for nimbolide's activity. Synthetic isomers of nimbolide vary in C ring size and stereochemistry (**40, 49**) all demonstrate only slightly lower cytotoxicity compared to nimbolide. However, isomer **41**, with a rearranged scaffold in C and D ring, is totally inactive. With these information, we then set out to synthesize analogues varying in E ring, aiming to substitute the potential metabolically labile furan group[55] as well as to improve the activity. Compound **47**, without the furan ring, demonstrates a 5x reduction in activity. With various functional groups installed in the cyclopentenone unit, our synthetic route worked smoothly under current conditions, affording analogues with 5 or 6-member C rings and different E rings. The phenyl-substituted analogues **51**–**53**, show a similar or improved bioactivity, which indicates furan moiety is replaceable. The additional cyclohexyl replaced analogues **54**–**56** were prepared and explored, and their comparable cellular activities suggest the π system was not required for its activity. the *para*-methoxy phenyl substituted (**57**–**59**) and *para*-OTBS phenyl substituted analogues (**63-65**) exhibited superior activities. We hypothesized that the *para*-methoxy and OTBS substituted phenyl group shall demonstrate a larger blocking area outside the RING domain of RNF114, and therefore increased cytotoxic potency was anticipated.

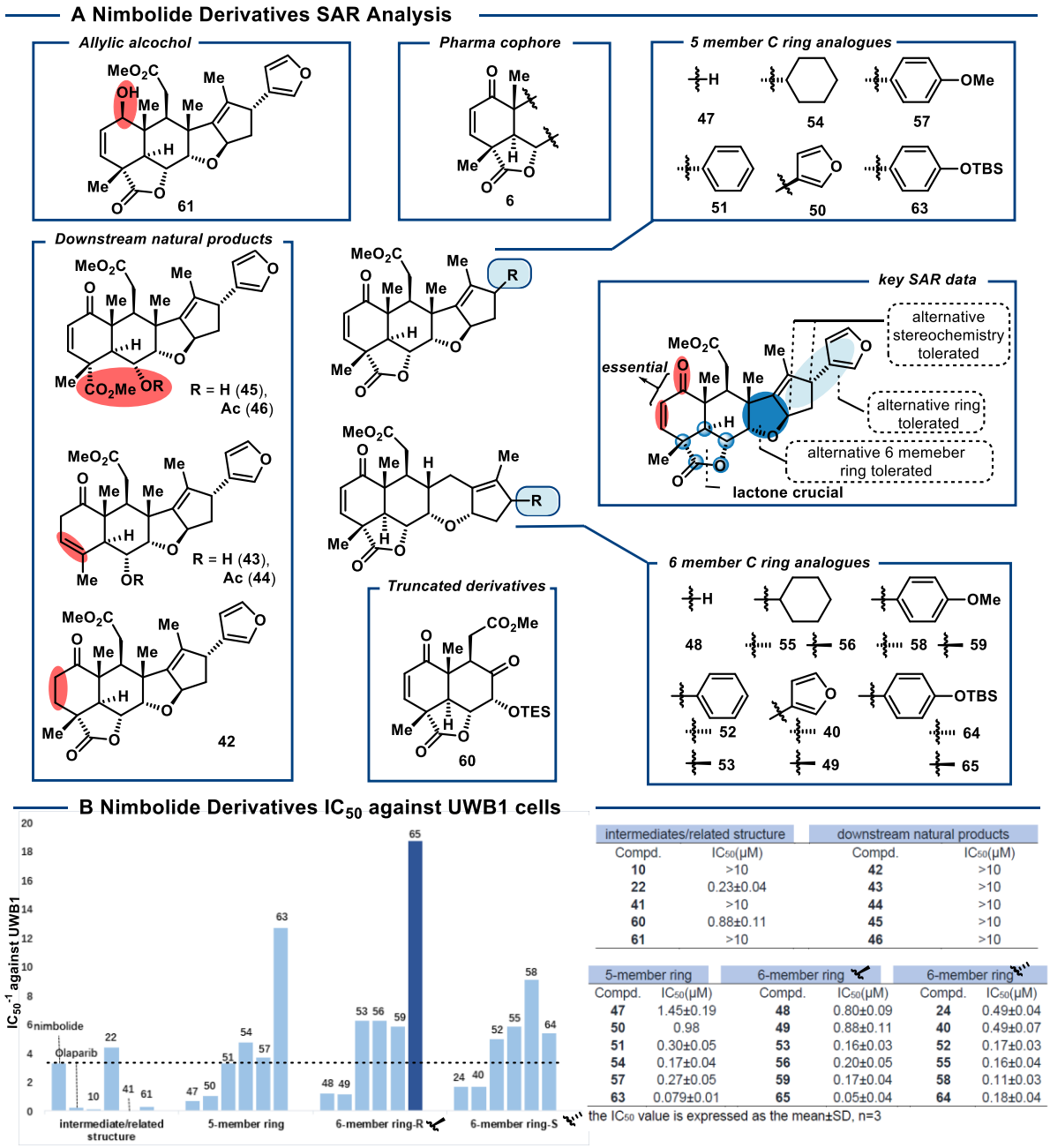

intermediates/related structure		downstream natural products	
Compd.	IC50(μM)	Compd.	IC50(μM)
10	>10	**42**	>10
22	0.23±0.04	**43**	>10
41	>10	**44**	>10
60	0.88±0.11	**45**	>10
61	>10	**46**	>10

5-member ring		6-member ring		6-member ring	
Compd.	IC50(μM)	Compd.	IC50(μM)	Compd.	IC50(μM)
47	1.45±0.19	**48**	0.80±0.09	**24**	0.49±0.04
50	0.98	**49**	0.88±0.11	**40**	0.49±0.07
51	0.30±0.05	**53**	0.16±0.03	**52**	0.17±0.03
54	0.17±0.04	**56**	0.20±0.05	**55**	0.16±0.04
57	0.27±0.05	**59**	0.17±0.04	**58**	0.11±0.03
63	0.079±0.01	**65**	0.05±0.04	**64**	0.18±0.04

the IC50 value is expressed as the mean±SD, n=3

Figure 5. Synthetic nimbolide analogs and their potency activity. A) nimbolide synthetic analogues SAR analysis; **B**) IC_{50} potency activity against UWB1 cells. See the Supplementary information for analogue preparation and experimental details.

After obtaining a number of potent analogues, their biological activity was subsequently investigated and re-validated. In this case, we focused on whether the PARP1 could still be efficiently trapped at the DNA damage site by few selective nimbolide analogs, and whether their cytotoxicity is correlated with the trapping capability. We therefore used the laser micro-irradiation experiments to examine PARP1 trapping (Figure 6). After DNA damage, the PARP1-GFP would accumulate around the DNA damage area (see Supporting Information for experiment details). In the DMSO control samples, the accumulation of PARP1 at DNA lesions reaches its peak after 30s and faded to the normal background in 10 mins. Two synthetic analogues, along with olaparib and nimbolide, with various cellular cytotoxicities were tested using this laser micro-irradiation experiment. Gratifyingly, we observed a positive correlation between their cytotoxicities and their PARP1 trapping activities. Notably, there was no PARP1 trapping in the RNF114 KO cells under treatment of nimbolide.[20]

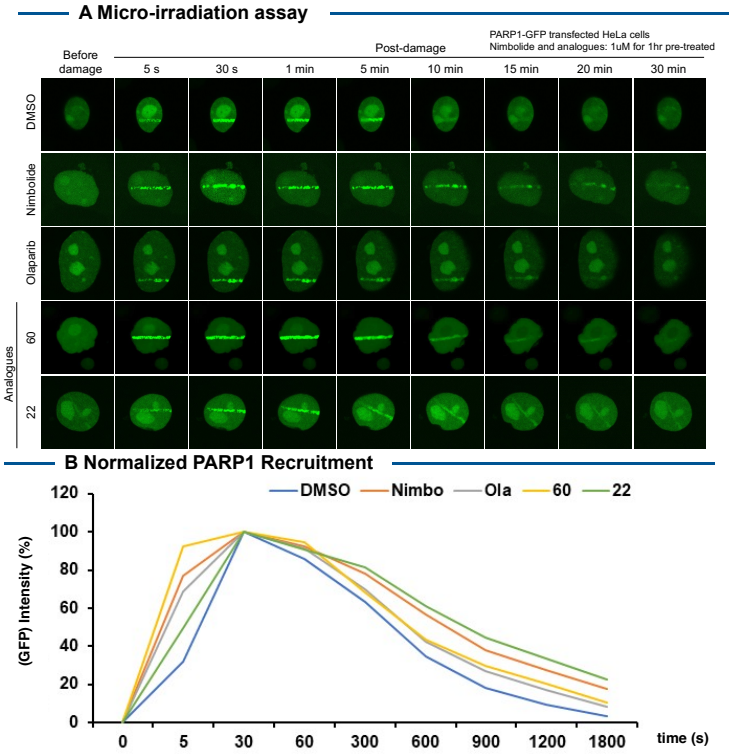

Figure 6. Olaparib, nimbolide and its analogs laser micro-irradiation assay. A) Laser micro-irradiation initiated PARP trapping assay; **B**) Normalized PARP1 recruitment data based on GFP intensity. GFP signals were monitored and were quantified in a time-course experiment. Set 30s PARP1 trapping as maximal recruitment.

In conclusion, the collection of a novel and validated MOA of nimbolide, and a convergent pharmacophore-directed late-stage coupling strategy to access nimbolide uniquely positions us towards translating these findings towards a next generation PARP1-targeting program for the treatment of *BRCA*-deficient cancers. As illustrated in Figure 2-5, this modular approach enables rapid and diverse preparation of nimbolide, related limonoids natural products, and synthetic derivatives. Their downstream biological activities have been investigated and more potent synthetic analogues were identified. Synergistic application (Figure 6) with laser micro-irradiation experiments allowed for rapid target re-validation and set the platform for further structure-activity relationship studies. As a result, the synthetic route enables the very exciting possibility of exploring and identifying novel nimbolide analogs as the second generation PARP1-targeting agents, potentially with a more complete and sustained response, against *BRCA*-deficient cancers.

References:

1. Sung, H. *et al.* Global Cancer Statistics 2020: GLOBOCAN Estimates of Incidence and Mortality Worldwide for 36 Cancers in 185 Countries. *CA. Cancer J. Clin.* **71**, 209–249 (2021).
2. Huang, A., Garraway, L. A., Ashworth, A. & Weber, B. Synthetic lethality as an engine for cancer drug target discovery. *Nat. Rev. Drug Discov.* **19**, 23–38 (2020).
3. Bryant, H. E. *et al.* Specific killing of BRCA2-deficient tumours with inhibitors of poly(ADP-ribose) polymerase. *Nature*. **434**, 913–917 (2005).
4. Farmer, H. *et al.* Targeting the DNA repair defect in BRCA mutant cells as a therapeutic strategy. *Nature.* **434**, 917–921 (2005).

5. Lord, C. J. & Ashworth, A. PARP inhibitors: Synthetic lethality in the clinic. *Science*. **355**, 1152–1158 (2017).

6. Chan, C. Y., Tan, K. V. & Cornelissen, B. PARP inhibitors in cancer diagnosis and therapy. *Clin. Cancer Res.* **27**, 1585–1594 (2021).

7. Chambon, P., Weill, J. D. & Mandel, P. Nicotinamide mononucleotide activation of a new DNA-dependent polyadenylic acid synthesizing nuclear enzyme. *Biochem. Biophys. Res. Commun.* **11**, 39–43 (1963).

8. Kraus, W. L. PARPs and ADP-Ribosylation: 50 Years … and Counting. *Mol. Cell.* **58**, 902–910 (2015).

9. Pommier, Y., O'Connor, M. J. & De Bono, J. Laying a trap to kill cancer cells: PARP inhibitors and their mechanisms of action. *Sci. Transl. Med.* **8**, 362ps17-362ps17 (2016).

10. Murai, J. *et al.* Trapping of PARP1 and PARP2 by clinical PARP inhibitors. *Cancer Res.* **72**, 5588–5599 (2012).

11. S. Wang *et al.* Uncoupling of PARP1 trapping and inhibition using selective PARP1 degradation. *Nat. Chem. Biol.* **15**, 1223–1231 (2019).

12. Kim, C., Wang, X.-D. & Yu, Y. PARP1 inhibitors trigger innate immunity via PARP1 trapping-induced DNA damage response. *Elife*. **9**, e60637 (2020).

13. Hopkins, T. A. *et al.* PARP1 trapping by PARP inhibitors drives cytotoxicity in both cancer cells and healthy bone marrow. *Mol. Cancer Res.* **17**, 409–419 (2019).

14. Ashworth, A. & Lord, C. J. Synthetic lethal therapies for cancer: what's next after PARP inhibitors? *Nat. Rev. Clin. Oncol.* **15**, 564–576 (2018).

15. Rodrigues, T., Reker, D., Schneider, P. & Schneider, G. Counting on natural products for drug design. *Nat. Chem.* **8**, 531–541 (2016).

16. Dias, D. A., Urban, S. & Roessner, U. A historical overview of natural products in drug discovery. *Metabolites*. **2**, 303–336 (2012).

17. Nicolaou, K., & Montagnon, T. Molecules that changed the world. *(Wiley-VCH, 2008)*.

18. Li, Q. *et al.* Synthetic group A streptogramin antibiotics that overcome Vat resistance. *Nature*. **586**, 145–150 (2020).

19. Murphy, S. K., Zeng, M. & Herzon, S. B. A modular and enantioselective synthesis of the pleuromutilin antibiotics. *Science*. **356**, 956–959 (2017).

20. Li, P. *et al.* Nimbolide Targets RNF114 to Induce the Trapping of PARP1 and Poly-ADP-Ribosylation-Dependent DNA Repair Factors. *bioRxiv* 2022.10.04.510815. doi: https://doi.org/10.1101/2022.10.04.510815

21. Spradlin, J. N. *et al.* Harnessing the anti-cancer natural product nimbolide for targeted protein degradation. *Nat. Chem. Biol.* **15**, 747–755 (2019).

22. Ekong, D. E. U. Chemistry of the meliacins (limonoids). The structure of nimbolide, a new meliacin from Azadirachta indica. *Chem. Commun. Lond.*, 808a–808a (1967).

23. Breslin, C. *et al.* The XRCC1 phosphate-binding pocket binds poly (ADP-ribose) and is required for XRCC1 function. *Nucleic Acids Res.* **43**, 6934–6944 (2015).

24. Renata, H., Zhou, Q. & Baran, P. S. Strategic Redox Relay Enables A Scalable Synthesis of Ouabagenin, A Bioactive Cardenolide. *Science.* **339**, 69–63 (2013).

25. Logan, M. M., Toma, T., Thomas-Tran, R. & Du Bois, J. Asymmetric Synthesis of Batrachotoxin: Enantiomeric Toxins Show Functional Divergence against Nav. *Science.* **354**, 865–869 (2016).

26. Jorgensen, L. et al. 14-Step Synthesis of (+)-Ingenol from (+)-3-Carene. *Science*. **341**, 878–882 (2013).

27. Wan, K. K. & Shenvi, R. A. Conjuring a supernatural product–delmarine. *Synlett*. **27**, 1145–1164 (2016).

28. Abbasov, M. E. *et al.* Simplified immunosuppressive and neuroprotective agents based on gracilin A. *Nat. Chem.* **11**, 342–350 (2019).

29. Veitch, G. E., Boyer, A. & Ley, S. V. The Azadirachtin Story. *Angew. Chem. Int. Ed.* **47**, 9402–9429 (2008).

30. Veitch, G. E. *et al.* Synthesis of Azadirachtin: A Long but Successful Journey. *Angew. Chem. Int. Ed.* **46**, 7629–7632 (2007).

31. Li, F.-Z. *et al.* A chiral pool approach for asymmetric syntheses of (−)-antrocin, (+)-asperolide C, and (−)-trans-ozic acid. *Chem. Commun.* **52**, 12426–12429 (2016).

32. Hamulic, D. *et al.* Synthesis and biological studies of (+)-liquiditerpenoic acid A (abietopinoic acid) and representative analogues: SAR studies. *J. Nat. Prod.* **82**, 823–831 (2019).

33. Michl, G., Rettenbacher, C. & Haslinger, E. Synthesis of 12-methoxyabietic acid methylester, a feeding deterrent of the larch sawflyPristiphora erichsonii (Hartig). *Monatshefte Für Chem. Chem. Mon.* **119**, 833–838 (1988).

34. Pelletier, S. W., Iyer, K. N. & Chang, C. W. Oxidative degradation of resin acids. *J. Org. Chem.* **35**, 3535–3538 (1970).

35. Larock, R. C., Hightower, T. R., Kraus, G. A., Hahn, P. & Zheng, D. A simple, effective, new, palladium-catalyzed conversion of enol silanes to enones and enals. *Tetrahedron Lett.* **36**, 2423–2426 (1995).

36. Kawamura, S., Chu, H., Felding, J. & Baran, P. S. Nineteen-step total synthesis of (+)-phorbol. *Nature*. **532**, 90–93 (2016).

37. Curci, R., D'Accolti, L. & Fusco, C. A novel approach to the efficient oxygenation of hydrocarbons under mild conditions. Superior oxo transfer selectivity using dioxiranes. *Acc. Chem. Res.* **39**, 1–9 (2006).

38. Kawamata, Y. *et al.* Scalable, electrochemical oxidation of unactivated C–H bonds. *J. Am. Chem. Soc.* **139**, 7448–7451 (2017).

39. Aranda, G. *et al.* Practical and Efficient 1α-Hydroxylation of 4,4Dimethyl2Ene Derivatives in Terpenic Series. *Synth. Commun.* **27**, 45–60 (1997).

40. Barluenga, J., Barrio, P., Riesgo, L., López, L. A. & Tomás, M. A general and regioselective synthesis of cyclopentenone derivatives through nickel (0)-mediated [3+2] cyclization of alkenyl Fischer carbene complexes and internal alkynes. *J. Am. Chem. Soc.* **129**, 14422–14426 (2007).

41. Ohashi, M., Taniguchi, T. & Ogoshi, S. Nickel-Catalyzed Formation of Cyclopentenone Derivatives via the Unique Cycloaddition of α,β-Unsaturated Phenyl Esters with Alkynes. *J. Am. Chem. Soc.* **133**, 14900–14903 (2011).

42. Jenkins, A. D., Herath, A., Song, M. & Montgomery, J. Synthesis of cyclopentenols and

cyclopentenones via nickel-catalyzed reductive cycloaddition. *J. Am. Chem. Soc.* **133**, 14460–14466 (2011).

43. Ahlin, J. S., Donets, P. A. & Cramer, N. Nickel (0)-Catalyzed Enantioselective Annulations of Alkynes and Arylenoates Enabled by a Chiral NHC Ligand: Efficient Access to Cyclopentenones. *Angew. Chem.* **126**, 13445–13449 (2014).
44. Shi, X., Gorin, D. J. & Toste, F. D. Synthesis of 2-Cyclopentenones by Gold(I)-Catalyzed Rautenstrauch Rearrangement. *J. Am. Chem. Soc.* **127**, 5802–5803 (2005).
45. Sha, C.-K. & Huang, S.-J. Synthesis of β-substituted α-iodocycloalkenones. *Tetrahedron Lett.* **36**, 6927–6928 (1995).
46. Barluenga, J., Tomás-Gamasa, M., Aznar, F. & Valdés, C. Straightforward Synthesis of Ethers: Metal-Free Reductive Coupling of Tosylhydrazones with Alcohols or Phenols. *Angew. Chem. Int. Ed.* **49**, 4993–4996 (2010).
47. Chandrasekhar, S., Rajaiah, G., Chandraiah, L. & Swamy, D. N. Direct conversion of tosylhydrazones to tert-butyl ethers under Bamford-Stevens reaction conditions. *Synlett*. **2001**, 1779–1780 (2001).
48. Crossley, S. W., Obradors, C., Martinez, R. M. & Shenvi, R. A. Mn-, Fe-, and Co-catalyzed radical hydrofunctionalizations of olefins. *Chem. Rev.* **116**, 8912–9000 (2016).
49. Nicolaou, K. C. *et al.* Studies toward the Synthesis of Azadirachtin, Part 2: Construction of Fully Functionalized ABCD Ring Frameworks and Unusual Intramolecular Reactions Induced by Close-Proximity Effects. *Angew. Chem. Int. Ed.* **44**, 3447–3452 (2005).
50. Overman, L. E., Abelman, M. M., Kucera, D. J., Tran, V. D. & Ricca, D. J. Palladium-catalyzed, polyene cyclizations: *Pure Appl. Chem.* **64**, 1813–1819 (1992).
51. Green, S. A., Huffman, T. R., McCourt, R. O., Puyl, V. van der & Shenvi, R. A. Hydroalkylation of Olefins To Form Quaternary Carbons. *J. Am. Chem. Soc.* **141**, 7709–7714 (2019).
52. Cui, B. *et al.* Limonoids from Azadirachta excelsa. *Phytochemistry.* **47**, 1283–1287 (1998).
53. Bokel, M., Cramer, R., Gutzeit, H., Reeb, S. & Kraus, W. Tetranortriterpenoids related to nimbin and nimbolide from Azadirachta indica A. Juss (Meliaceae). *Tetrahedron.* **46**, 775–782 (1990).
54. Kraus, W. & Cramer, R. Pentanortriterpenoide aus Azadirachta indica A. Juss (Meliaceae). *Chem. Ber.* **114**, 2375–2381 (1981).
55. Peterson, L. A. Reactive Metabolites in the Biotransformation of Molecules Containing a Furan Ring. *Chem. Res. Toxicol.* **26**, 1, 6–25 (2013).

Acknowledgements

Financial support for this work was provided by Welch Foundation (I-2010-20190330 to T.Q., and I-1800 to Y.Y.), National Institutes of Health (R01GM141088 to T.Q., 5R35GM134883, 1R01NS122533 and 1R21CA261018 to Y.Y.) and UT Southwestern Eugene McDermott Scholarship (T.Q.). We thank Feng Lin (UTSW) for assistance with NMR spectroscopy; Hamid Baniasadi (UTSW) for HRMS; Vincent Lynch (UT-Austin) for X-ray crystallographic

analysis. We thank the Prof. Uttam Tambar (UT Southwestern) for generous access to chiral HPLC equipment, Prof. Phil Baran (Scripps Research) for helpful discussions.

Author Contributions

H.D., H.D. and T.Q. performed synthetic experiments; C.K., P.L., X.W. performed the cellular potency and micro-irradiation experiments; Y.Y. and T.Q. designed and supervised the project; all authors wrote the paper.

Competing Interests

Patents have been filed on some aspects of the work in this manuscript, and H.D., H.D., C.K., P.L., Y.Y. and T.Q. are listed as inventors; Y.Y. and T.Q. are co-founders and shareholders of ProteoValent Therapeutics.

Data Availability

Experimental procedures, alternative synthetic route, optimization data, ^{1}H NMR spectra, ^{13}C NMR spectra and MS data are available in the Supplementary Materials.